Modeling and Control of DSTATCOM with BESS for Mitigation of Flicker

Vasudeo B. Virulkar [1] Mohan V. Aware [2]

Abstract – Industry customers of supply utility such as, electric arc furnaces and arc resistance welder and other such time varying loads which are cyclic in nature are the major flicker source to influence the grid power quality. Distribution STATic Synchronous COMpensator (DSTATCOM) with Battery Energy Storage System (BESS) is proposed as a viable and effective alternative for mitigation of flicker.

This paper examines the dynamic performance of a DSTATCOM coupled with BESS for mitigation of flicker. The detailed modeling of DSTATCOM with BESS and its control strategies are analyzed. The control technique proposed will be focused on the control of energy flow among the system components with effective real power utilization from the batteries. This relives the main power system components from the fluctuating voltages. The detail components of the systems are mathematically modeled to embed the battery energy for the real power utilization to mitigate the voltage fluctuations. Results from digital simulation performed in PSCAD/EMTDC will demonstrate the effectiveness of DSTATCOM/BESS for mitigation of flicker.

Keywords – Battery energy storage (BESS), control techniques, custom power devices, Distribution STATic Synchronous COMpensator (DSTATCOM), Electric Arc Furnace, Flicker

I. INTRODUCTION

Recently, with the growth of industry manufacturers and population, electric power quality becomes more and more important. As one of the most power quality issues, flicker due to feeder voltage fluctuation, influences domestic lighting and sensitive apparatus of nearby transmission and distribution system. Electric arc furnace (EAF), as a major industry customer of supply utility, consumes considerable real power and reactive power with the time-varying, stochastic and even chaotic characteristics during melting and refining process, and therefore generates severe flicker to the grid [1]. There are other industrial applications where high power are switched on and off with a period less than 0.5 s. During the switching on and off of these loads, the demanded high currents determine a voltage drop across the line impedance which is responsible for voltage fluctuations. Voltage fluctuation causes an annoying variation in the output illumination from incandescent or fluorescent lamps. The severity of the annoyance is generally dependent on the frequency and amplitude of the voltage variation and the short circuit capacity of the PCC.

The paper first received 1 Sep 2009 and in revised form 1 Jan 2010.
Digital Ref: A170601238
[1] Department of Electrical Engineering, Visvesvaraya National Institute of Technology, Nagpur (India) E-mail: vbvirulkar@yahoo.com.
[2] Department of Electrical Engineering, Visvesvaraya National Institute of Technology, Nagpur (India) E-mail: mva_win@yahoo.com.

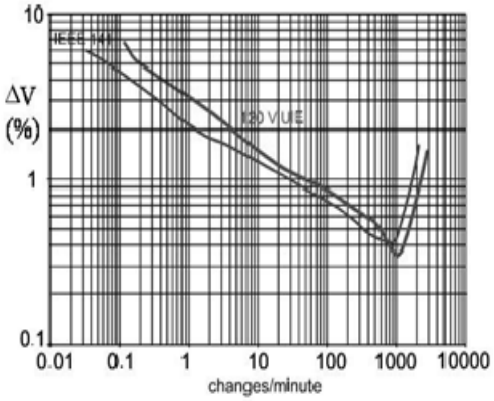

Fig. 1: Maximum permissible voltage fluctuation

It is reported that a small voltage fluctuation of less than 0.5% in the frequency range of 5-10 Hz can cause a visible and uncomfortable incandescent flicker [2]. In addition to the perceptible and sometimes irritating lighting flicker to humans, voltage flicker can also cause electrical equipment efficiency drop, torque and power oscillations, and interference in protection systems. Now a day, consumers require high quality power supply for their sensitive loads. Voltage flicker has therefore been an important power quality concern for Supply utilities, regulatory agencies and customers. To quantify the degree of voltage flicker and its mitigating solutions various definitions and standards have been proposed. The IEEE Standard 1453-2004 [3], which is referred widely, defines maximum permissible voltage flicker levels with respect to frequency as shown in Fig. 1.

Just as flexible as transmission systems (FACTS) controllers are used to improve the quality and reliability of transmission systems, these devices can be used in the distribution system known as custom power devices with significant benefits of bringing the solution to the wide range of problems belonging to the quality and reliability of power that is delivered to the customers [4].
A distribution static compensator or DSTATCOM is a fast response, solid-state power controller that provides flexible voltage control at the point of coupling (PCC) to the utility distribution feeder for mitigations of power quality problem. If it is coupled with energy storage system (ESS), it can exchange both active and reactive power with the distribution system by varying the amplitude and phase angle of the converter voltage with respect to the system voltage. The result is a controlled current flow through the interfacing inductance between DSTATCOM and the distribution system. This enables the DSTATCOM to mitigate voltage fluctuations of the distribution system in instantaneous real-time [5].

This paper discusses the dynamic performance of DSTATCOM with BESS for mitigation of flicker. Modeling and control approaches are proposed, including the detailed modeling of DSTATCOM/BESS device.

Validation of model and control approach is carried out through simulation by using PSCAD/EMTDC.

II. EAF FLICKER MODEL

The Arc furnace operation is a complicated dynamic arcing process. Historically, there are various methods to model arc furnace, such as arcing resistance model, harmonics accumulation model and frequency domain method [6]-[7]. These methods can match the non-linear v-i curve, stochastic and even chaotic characteristics of EAF, therefore, they are satisfactory for the purpose of power quality analysis. However, from the flicker mitigation point of view, a deterministic model needs to be developed.

A. Arc Furnace Model

The arc melting process is a very complicated process, it transfer the electric energy to thermal energy. The random movement of the melting material results in the electrical and thermal dynamics during the arc melting process, thus no two cycles of the arc voltage and current waveforms are identical. By examining the actual V-I characteristic of the arc furnace, in general the arc melting process can be divided into three periods. For convenience of study, some approximations are made according to these three periods, which are explained below.

- In the first period, the arc begins to reignite from extinction. When the arc voltage increases to zero, the arc current also reaches its zero crossing point. As the arc voltage increases to the reignition voltage V_{ig}, the equivalent circuit acts as an open circuit. However, small leakage current exits, which flows throw the floamy slag parallel with the arc. The floamy slag is assumed to be proportional to the arc length.
- In the second period, the arc is established. A transient process appears in the voltage waveform at the beginning of arc melting process. The arc voltage drops suddenly from V_{ig} to a constant value V_d. This process is assumed to be expressed as an exponential function with a time constant τ_1.
- During the third period, the arc begins to extinguish. The arc voltage continues to drop smoothly, except a sharp change after the arc extinction. This process is also assumed to be represented by an exponential function with a time constant τ_2.

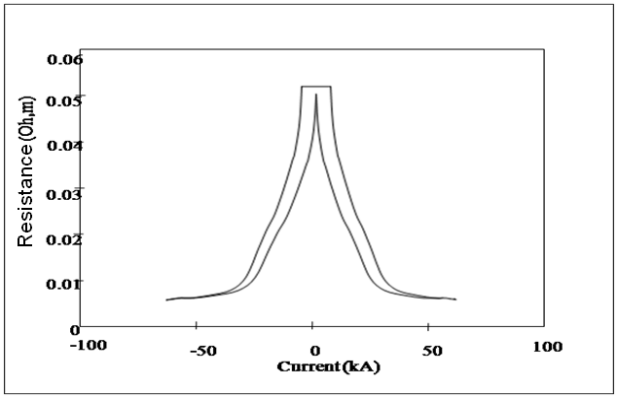

Fig. 2: Current Resistance Curve

Following the above approximation, the arc model can be expressed in the form of current controlled nonlinear resistance as shown in Fig. 2 can be represented by (1)

$$R_a = \begin{cases} R_g & 0 < |i| < i_g \\ & and \ \dfrac{d|i(t)|}{dt} > 0 \\ (V_d + (V_{ig} - V_d) & |i| \geq i_{ig} \\ e^{-(|i|-i_g)/\tau_1}) / |i|; & and \ \dfrac{d|i(t)|}{dt} > 0 \\ \left(V_t + (V_{ig} - v_t)e^{-|i|/\tau_2}\right) & \dfrac{d|i(t)|}{dt} \prec 0 \\ / \left(|i| + i_{ig}\right); & \end{cases} \quad (1)$$

with the continuous condition of the arc resistance at the maximum current value I_{max} and the exponential formulas, some parameters in (1) are calculated as (2);

$$\begin{cases} V_{ig} 1.15 * V_d \\ i_{ig} = \dfrac{V_{ig}}{R_g} \\ Vt = \dfrac{\mathrm{I}_{max} + i_{ig}}{\mathrm{I}_{max}} V_d \end{cases} \quad (2)$$

Normally, the average arc voltage V_d has a linear relationship with the average arc length l, that is,

$$V_d = A + Bl \quad (3)$$

where A and B are constants [8]. Thus, the nonlinear resistance is controlled by the arc length.

As shown in Fig. 3, a flicker model consisting of switching passive loads is proposed to model EAF flicker under worst case condition. This behavior model can represent similar impedance as real-world EAF and therefore produces similar flicker at PCC. From the real-time recorded waveform of EAF, the flicker can be summarized as below: (1) The flicker frequency: around 5Hz; (2) The flicker magnitude *(ΔV/V)*: around 1%; (3) Source *Xs/Rs*; around 3 [9].

Since the 1% flicker is beyond the IEEE irritability threshold curve of IEEE standard [9], the mitigation device has to be applied to mitigate the flicker to an acceptable range. From power flow point of view, the basic principle of flicker mitigation solution can be simply explained as shown in Fig. 4. The power consumed by EAF can be regarded as a constant power (P_0, Q_0) plus a fluctuating power (ΔP, ΔQ).

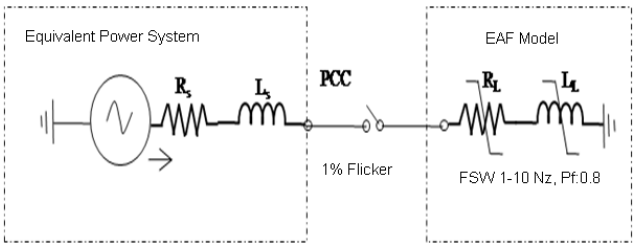

Fig. 3: Worst Case Flicker Model of Electric Arc Furnace

III. FLICKER MITIGATION SOLUTIONS

Generally, P_0 affects the angle stability, load power factor and ΔP is mainly related to the fluctuations of bus voltage magnitude. To solve the EAF power quality issues, ideally,

it is obvious to compensate Q_0, ΔP and ΔQ so that the supply only provides the constant P_0 with unity power factor, and, thereby, the bus voltage magnitude and angle is kept constant.

However, because of cost-effectiveness and other factors, Q_0, ΔP and ΔQ cannot be fully compensated, but only mitigated to an acceptable level in the real world. Particularly, ΔP mainly affects the voltage angle other than flicker and requires energy storage source for compensation. Flicker Mitigation techniques can be classified into three types: (1) Passive filters, which can be either series or shunt [11].
The passive filters are simple, reliable, low-cost and highly efficient, it is difficult to design for a stiff system, time consuming for tuning, easy to induce resonance, and not, susceptible to system impedance variations. (2) Series active compensators, such as series impedance regulation [12].

Although, increasing series reactance mitigates the flicker to some extent, it results in voltage reduction and consequently EAF productivity. Moreover, it is also expensive and cumbersome to control the upstream transformer reactance in today's deregulated power system. (3) Shunt active compensator, such as SVC and STATCOM. SVC can improve the power quality and increase the EAF productivity leading to additional economic benefits. However, it cannot react to the fast varying flicker (1Hz-20Hz) very well within the inherent limit of relatively low bandwidth and its dynamic performance for flicker mitigation is limited. The state-of-art solution is the DSTATCOM based on high frequency switching voltage source converter (VSC). While SVC performs as controlled reactance admittance, DSTATCOM functions as synchronous voltage source. The DSTATCOM response time is less than one cycle and follows the fast changing flicker well [13].

IV. Modeling of the DSTATCOM/BESS

A. Modeling of DSTATCOM

A DSTATCOM consists of three-phase six pulse voltage source inverter (VSI) shunt connected to the distribution network by means of coupling transformer with the ability to both generate and absorb reactive and active power.

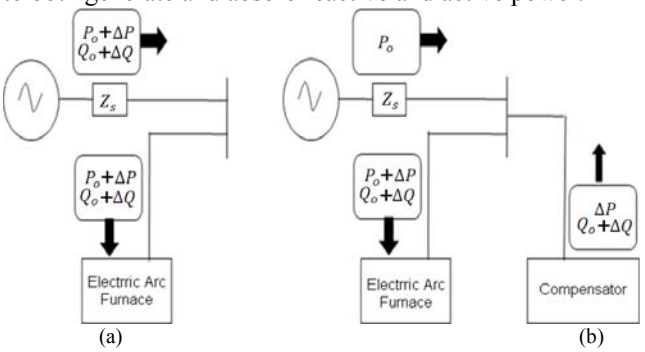

Fig. 4: Electric Arc Furnace (a) without compensator (b) With compensator

The reactive power exchange between the AC system and the DSTATCOM is controlled varying the magnitude of the fundamental component of the inverter voltage above and below that of AC system; this is achieved by small variations in the switching angle of the semiconductor devices. When the voltage's fundamental component produced by the inverter is forced to lag or lead the AC system voltage by a few degrees, an active power may flow into or out of the inverter modifying the DC capacitor voltage value. Otherwise, if the inverter supplies only reactive power, the active power provided by the capacitor is zero, therefore the DC capacitor does not modify its voltage.

The schematic diagram of a voltage source converter is shown in Fig. 5.
The ac source voltages are e_a,e_b,and e_c. The ac currents are i_a, i_b, and i_c. The ac terminal voltages of the converter are v_a, v_b, and v_c. The dc voltage and current are V_{dc} and I_{dc}, respectively.

The ac side impedance is modeled as an inductor L in series with a resistor R. The dc side capacitor is C_{dc}. And the dc load is R_{dc}. The converter is controlled under sinusoidal PWM technique. The modulation signal of phases a, b, and c are m_a, m_b, and m_c, respectively. The relationship between the fundamental components of the ac terminal voltages v_a, v_b, v_c, and the dc voltage V_{dc} is

$$v_a = \frac{1}{2} m_a V_{dc}; \quad v_b = \frac{1}{2} m_b V_{dc}; \quad v_c = \frac{1}{2} m_c V_{dc}; \tag{4}$$

Taking the ac source voltage as the reference phasor, the conventional dynamic equation in d-q coordinates are

$$\frac{d}{dt} V_{dc} = -\frac{1}{R_{dc} C_{dc}} V_{dc} + \frac{3}{2C_{dc}} M_d I_d \tag{5}$$

$$\frac{d}{dt} I_d = -\frac{R}{L} I_d + \omega I_q - \frac{1}{2L} M_d V_{dc} + \frac{1}{L} E_d \tag{6}$$

$$\frac{d}{dt} I_q = -\omega I_d - \frac{R}{L} I_q - \frac{1}{2L} M_q V_{dc} \tag{7}$$

Where V_{dc}, I_d, and I_q are the state variables, M_d, and M_q are the inputs, and V_{dc} and I_q are outputs, and E_d is a constant.
Obviously, (5)-(7) represents a nonlinear system and it is not easy to design a controller for such a system. However, the above system can be modified to a linear system through a set of non-linear transformations. The power consumed on the dc-side can be expressed as

$$P_{dc} = V_{dc} C_{dc} \frac{d}{dt} V_{dc} + \frac{V_{dc}^2}{R_{dc}} \tag{8}$$

The power delivered from the ac side can be written as

$$P_{ac} = \frac{3}{2} E_d I_d \tag{9}$$

The power delivered from the ac side can be written as

$$P_{ac} = \frac{3}{2} E_d I_d \tag{10}$$

If the ac side resistor R is very small, the power loss in R can be neglected. In most applications, this assumption is valid. Therefore, from (8) and (9)

If (V_{dc}^2) is taken as a dynamic equation instead of (5). As a result, the original nonlinear system can now be written as

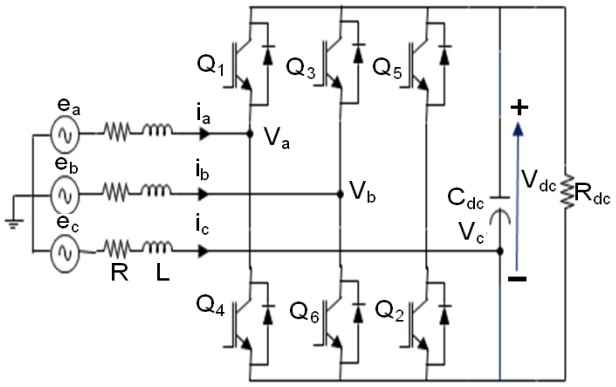

Fig. 5: Schematic Diagram of a Voltage Source Converter

$$\frac{d}{dt}\left(V_{dc}^2\right) = -\frac{2}{R_{dc}C_{dc}}\left(V_{dc}^2\right) + \frac{3E_d}{C_{dc}}I_d \tag{11}$$

$$V_{dc}C_{dc}\frac{d}{dt}V_{dc} + \frac{V_{dc}^2}{R_{dc}} = \frac{3}{2}E_dI_d \tag{12}$$

$$\frac{d}{dt}I_d = -\frac{R}{L}I_d + \omega I_q - \frac{1}{L}E_d \tag{13}$$

$$\frac{d}{dt}I_q = -\omega I_d - \frac{R}{L}I_q - \frac{1}{L}V_q \tag{14}$$

where $V_d = (1/2)M_dV_{dc}$ and $V_q = (1/2)M_qV_{dc}$ are the new inputs of the system. Equations (12) - (14) represent a linear model that describes the DSTATCOM.

In general, the DSTATCOM can be utilized for providing voltage regulation, power factor correction, harmonics compensation and load leveling [14]. The addition of energy storage through an appropriate interface to the custom power leads to more flexible integrated controller. The ability of the DSTATCOM/ESS of supplying effectively extra active power allows expanding its compensating actions, reducing distribution losses and enhancing the operation of the grid [15].

The presented VSI corresponds to a dc to ac switching power inverter using insulated Gate Bipolar Transistors (IGBT). In the distribution voltage level, the switching device is generally the IGBT due to its lower switching losses and reduced size. In addition, the rating of custom power devices is relatively low.
As a result the voltage control of DSTATCOM can be achieved by using high power fast-switched IGBTs. This topology supports the future use of PWM control even for high power applications.

The connection to the utility grid is made by using low pass sine wave filters in order to reduce the perturbation on the distribution system from high-frequency switching harmonics generated by PWM control. The total harmonic distortion (THD) of the output voltage of the inverter combined with sine wave filter is less than 5% at full rated unity power factor load. Typically, leakage inductance of the set up transformer windings is high enough as to build the sine wave filter simply by adding a bank of capacitors in the PCC. In this way, an effective filter is obtained at low cost, permitting to improve the quality of the voltage waveforms introduced by the PWM control to the power utility and meeting the power quality requirement [10].

A simplified scheme of the DSTATCOM/BESS equivalent circuit is shown in Fig. 6. The DSTATCOM is considered as a voltage source that shunt connected to the distribution network through inductance L_s, accounting for the equivalent leakage reactance of the set-up coupling transformer and the series resistance R_s, representing the transformer winding resistance and VSI semiconductor conduction losses. The mutual inductance M represents the equivalent magnetizing impedance of the set-up transformers. In the dc side, the capacitance of the dc bus capacitor is described by C_d whereas
the switching losses of the VSI and power loss in the capacitors are considered by R_p.
The dynamic equations governing the instantaneous values of the three-phase output voltage in the ac side of the DSTATCOM and the current exchanged with the distribution grid are given by (13) and (14).

$$\begin{bmatrix} v_{inv_a} \\ v_{inv_b} \\ v_{inv_c} \end{bmatrix} - \begin{bmatrix} v_a \\ v_b \\ v_c \end{bmatrix} = \left(R_s + sL_s\right)\begin{bmatrix} i_a \\ i_b \\ i_c \end{bmatrix} \tag{15}$$

where:

$$s = \frac{d}{dt}, R_s = \begin{bmatrix} R_s & 0 & 0 \\ 0 & R_s & 0 \\ 0 & 0 & R_s \end{bmatrix}, L_s = \begin{bmatrix} L_s & M & M \\ M & L_s & M \\ M & M & L_s \end{bmatrix} \tag{16}$$

Under the assumption that the system has no zero sequence components, all currents and voltages can be uniquely transformed into the synchronously-rotating *dq* reference frame. Thus, the new coordinate system is defined with the *d*-axis always coincident with the instantaneous reactive power.
By applying Park's transformation [16] (15) and (16) can be transformed into *dq* reference frame as follows:

$$\begin{bmatrix} v_{inv_d} - v_d \\ v_{inv_q} - v_q \\ v_{inv_0} - v_0 \end{bmatrix} = K_s\begin{bmatrix} v_{inv_a} - v_a \\ v_{invb_a} - v_b \\ v_{invc_a} - v_c \end{bmatrix}, \begin{bmatrix} i_d \\ i_q \\ i_0 \end{bmatrix} = K_s\begin{bmatrix} i_a \\ i_b \\ i_c \end{bmatrix} \tag{17}$$

where K_s is Park's transformation matrix given by

$$K_s = \sqrt{\frac{2}{3}}_s\begin{bmatrix} \cos\theta & \cos(\theta - 2\pi/3) & \cos(\theta + 2\pi/3) \\ \sin\theta & \sin(\theta - 2\pi/3) & \sin(\theta + 2\pi/3) \\ 1/\sqrt{2} & 1/\sqrt{2} & 1/\sqrt{2} \end{bmatrix} \tag{18}$$

then by neglecting the zero sequence components, (19) and (20) are derived.

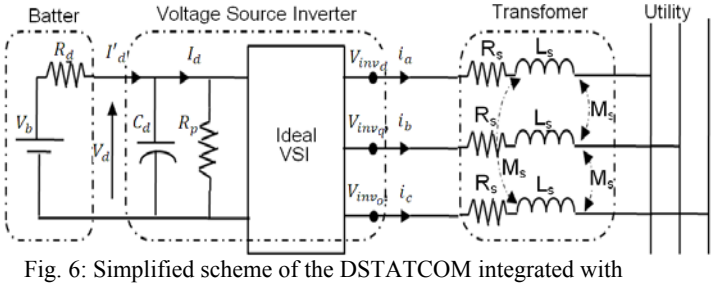

Fig. 6: Simplified scheme of the DSTATCOM integrated with BESS

$$\begin{bmatrix} v_{inv_d} \\ v_{inv} \end{bmatrix} - \begin{bmatrix} v_d \\ v_q \end{bmatrix} = (R_s + sL_s)\begin{bmatrix} i_d \\ i_q \end{bmatrix} + \begin{bmatrix} -\omega & 0 \\ 0 & \omega \end{bmatrix}L_s'\begin{bmatrix} i_d \\ i_q \end{bmatrix}, \tag{19}$$

Where:

$$R_s = \begin{bmatrix} R_s & 0 \\ 0 & R_s \end{bmatrix}, L_s' = \begin{bmatrix} L_s' & 0 \\ 0 & L_s' \end{bmatrix} = \begin{bmatrix} L_s - M & 0 \\ 0 & L_s - M \end{bmatrix} \tag{20}$$

B. Modeling of BESS

Various types of energy storage technologies can be incorporated into the dc bus of the DSTATCOM, namely superconducting magnetic energy storage (SMES), supercapacitores (SC), flywheel and battery energy storage system (BESS), among others. However, lead acid id batteries offer a more economical solution for application in the mitigation of flicker that require small devices for supplying power for small period of time and intermittently. The energy stored in a lead acid battery is chemical energy that is translated into electrical energy. Lead acid batteries are rechargeable and have the following reversible reaction: [17]

$$Pb + PbO_2 + 2H_2SO_4 \leftrightarrow 2PbSO_4 + 2H_2O \tag{21}$$

The battery voltage is related to the sum of the reduction and oxidation potentials. Electrical energy is produced when the chemicals in the battery react with the following conditions:

- State of charge
- Battery storage capacity
- Rate of charge/discharge
- Environmental temperature
- Age/Shell life

The battery model can be represented by an equivalent electric network as shown in Fig. 7 along with the dynamic equations representing the charge storage process and electrolyte heating

$$Q_e = \int_0^t -\mathrm{I_m}(\tau)d\tau \tag{22}$$

$$C_\theta \frac{d\theta}{dt} = \frac{\theta - \theta_e}{R_\theta} + P_s \tag{23}$$

Where:

Q_e so-called "extracted charge," i.e., the charge that has been actually extracted from the battery starting from the battery completely full (battery full when t=0);

C_θ and R_θ battery thermal capacitance and resistance, respectively;

P_s Heating power generated inside the battery by conversion from electrical or chemical energy.

It has to be remembered that the resistance R_k and capacitance C_k shown in Fig. 6 are function of the battery state-of-charge and electrolyte temperature.

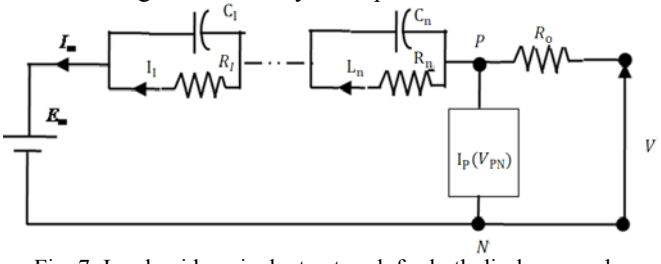

Fig. 7: Lead-acid equivalent network for both discharge and charge

The BESS as shown in Fig. 5 is represented by an ideal dc voltage source V_b and a series resistance R_b, accounting for battery internal resistance. The self-discharge and leakage as well as capacity of the batteries are represented by parallel combination of resistance and capacitor.

The DSTATCOM ac and dc sides are related by the power balance between the input and the output on an instantaneous basis as described by (24) and (25).

$$P_{ac} = P_{dc} \tag{24}$$

$$\frac{3}{2}\left(v_{inv_d} i_d + v_{inv_q} i_q\right) = \left(\frac{V_b - V_d}{R_d}\right) - C_d V_d \frac{dV_d}{dt} - \frac{V_d^2}{R_p} \tag{25}$$

The VSI of the DSTATCOM basically generates the ac voltage (v_{inv}) from the dc voltage (V_d). Thus, the onnection between the dc-side voltage and the generated ac voltage can be described by using the average witching function matrix S and the factor k_{inv} as given by (26) through (27).

$$\begin{bmatrix} v_{inv_d} \\ v_{inv_q} \end{bmatrix} = k_{inv} \begin{bmatrix} S_d \\ S_q \end{bmatrix} V_d, \tag{26}$$

with the factor:

$$k_{inv} = \frac{1}{2} ma \tag{27}$$

Being,

m: modulation index, $m \in [0, \quad 1]$,

$a = \frac{n_2}{n_1}$: voltage ratio of the coupling set-up transformer

And the average switching factor matrix for dq reference frame,

$$\begin{bmatrix} S_d \\ S_q \end{bmatrix} = \begin{bmatrix} \cos\alpha \\ \sin\alpha \end{bmatrix}, \tag{28}$$

with:

α: phase-shift of the converter output voltage from the reference position

Essentially, (16), (17) and (24) through (27) can be summarized in the state-space as follows.

$$s\begin{bmatrix} i_d \\ i_q \\ V_d \end{bmatrix} = \begin{bmatrix} \frac{-R_s}{L_s'} & \omega & \frac{k_{inv} S_d}{L_s'} \\ -\omega & \frac{-R_s}{L_s'} & \frac{k_{inv} S_q}{L_s'} \\ \frac{3}{C_d} k_{inv} S_d & \frac{3}{C_d} k_{inv} S_q & \frac{2}{C_d}\left(\frac{R_b R_p}{R_b + R_p}\right) \end{bmatrix} \begin{bmatrix} i_d \\ i_q \\ V_d \end{bmatrix} + \begin{bmatrix} \frac{|v|}{L_s'} \\ 0 \\ \frac{2}{R_b C_d} V_b \end{bmatrix} \tag{29}$$

IV. CONTROL STRATEGY

The operation of the DSTATCOM/BESS as a flicker mitigating component is achieved by a suitable control algorithm that manages the energy transfer among the BESS, dc-link capacitor, and the distribution system. The analysis of the energy control system (ECS) is based on the following assumptions. The control systems of the converter are able to keep the source power P_s and the BESS power P_{BESS} close to their reference, i.e. P_s^* and P_{BESS}^*;

Losses in the passive components such as inductors, capacitors, storage device, and in the static switches are neglected

These two assumptions are acceptable because of the low time response of the control system used to drive the converter and the small amount of the losses in the passive components. Furthermore, the time constant of the storage device must be low enough to allow the tracking of the energy variations demanded by the ECS. The analysis of

the ECS can be usefully carried out in terms of power flow and energy balance using the Laplacian notation [19]. The proposed control algorithm is shown scheme of Fig. 8. In this scheme the input control variables of the DSTATCOM/BESS are the energy in the dc-link capacitor E_C^* and the energy in the BESS E_{BESS}^*.

The controller R_1 generates the reference source power, which combined to the load power gives the reference DSTATCOM power. This has to be injected by the VSI into the PCC. At the same time, the controller R_2 generates the firing signals for the dc/dc chopper, which controls the power flowing into the storage device. The controller $R_3(s)$ varies the energy reference in the BESS on the basis of the error of the dc capacitor energy. Once the parameters of the controller R_1, R_2, and R_3 are defined, it is possible to determine the transfer function of the control loops represented in Fig. 9. The control algorithm has been designed to manage the transfer of energy between the BESS and the dc-link capacitor during the transient conditions caused by the load variations. In this way the ECS operates in order to recover the energy level in the capacitor, using a fraction of the energy stored in the BESS. During load changes, the energy variations in the capacitor are quickly compensated by the energy transfer between the BESS and the dc-link capacitor. Consequently, the energy required by the load can be considered as coming directly from the BESS. The source is not required to supply the full load power, but an increasing amount of power. The use of BESS to smooth the load variation is necessary because the dc link capacitor has very small amount of energy stored. Moreover, its energy variation must be minimized for correct operation of VSI with practically constant dc-link voltage.

Assuming the capacitor energy and the BESS energy are close to their references, respectively E_C^* and E_{BESS}^*, an increase of the load power P_L determines a power flow from the capacitor to the ac side, yielding an error $\Delta E_C = E_C^* - E_C$ in the capacitor stored energy.

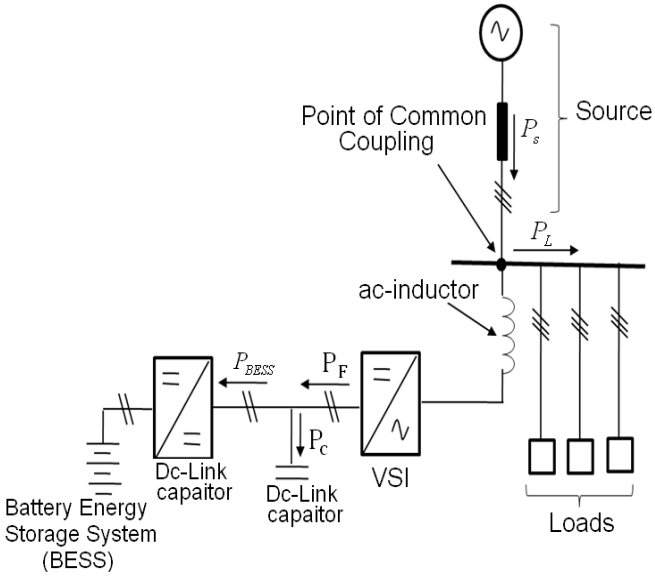

Fig. 8: Scheme of DSTATCOM/BESS System

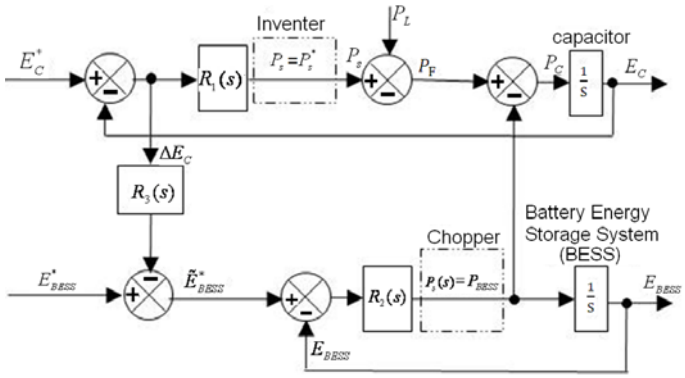

Fig. 9: Energy Control System

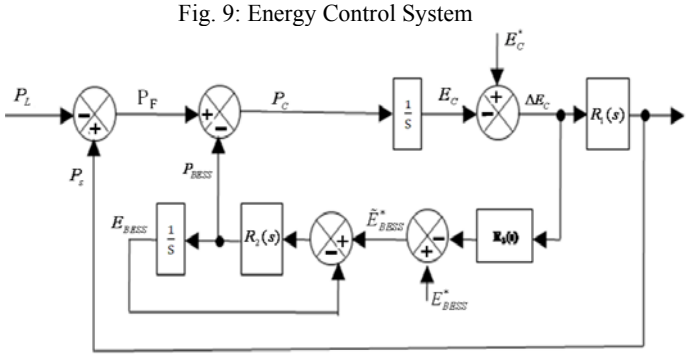

Fig. 10: Block Diagram showing the relationship between P_L and P_s

Assuming a simple proportional controller the new BESS energy reference will be given by:

$$\tilde{E}_{BESS}^* = E_{BESS}^* - K_{P3}\Delta E_C \tag{29}$$

This new lower value of the reference allows the chopper to recover the dc-link voltage using the energy stored in BESS.

A scheme shown in Fig. 8 is used to analyze the operation of DSTATCOM/BESS for mitigation of flicker due to pulsating loads. Analyzing the transfer function of the control loop given in Fig. 9 , the DSTATCOM/BESS can smooth the source power variation due to pulsating loads. The control scheme of Fig. 10 is derived from the basic scheme of Fig. 9 by considering the load power P_L as input signal, and the source power P_s as output variable.

The reference for the dc-link capacitor energy and for the BESS energy can be considered as disturbances having constant values. The relationship between the source power and the load power can be easily calculated assuming the controller of Fig. 3 with following expressions:

Capacitor energy controller:

$$R_1(s) = K_{P1} + \frac{K_{I1}}{s}$$

BESS energy controller:

$$R_2(s) = K_{P2}$$

BESS energy reference controller:

$$R_3(s) = K_{P3,}$$

With these assumptions the expression for $P_s(s)$ is given by the sum of three terms as represented in (17) and in Fig. 10.

$$P_s(s) = G_C(s)E_C^* + G_{BESS}(s)E_{BESS}^* + G_L(s)P_L \tag{30}$$

The expressions for $G_C(s), G_{BESS}(s), G_L(s)$ are given in Appendix. Under the assumption that E_C^* and E_{BESS}^* are constant, by applying final value theorem to the step response of the transfer function $G_L(s), G_{BESS}(s)$ yields

$$\begin{cases} \lim_{s\to 0} s\dfrac{1}{s} G_C(s) = 0 \\ \lim_{s\to 0} s\dfrac{1}{s} G_{BESS}(s) = 0 \end{cases} \quad (31)$$

This means that the relationship between the BESS power and the load power is given only by the transfer function $G_L(s)$. On the basis of this result, the analysis of the control system can be carried out with reference to the following open loop transfer function derived from $G_L(s)$,

$$G_{La}(s) = \frac{(K_{P1}s + K_{1I})(s + K_{P2})}{s^2(s + K_{P3}K_{P2})} \quad (32)$$

The resulting control system can be simplified as represented in Fig. 11. The parameters of the transfer function (32) must be tuned to obtain the desired behavior of the source power in response to the load power variation. A deep discharge of the BESS determines a greater amount of energy flowing from the DSTATCOM/BESS towards PCC, yielding to a longer time interval during which the DSTATCOM/BESS supplies the load power.

V. DIGITAL SIMULATION

For a 100 MVA Electric Arc Furnace connected to system of 34.5/0.9 kV is simulated in PSCAD/EMTDC with the 50 MVA DSTATCOM and 10 MW/10 s VRLA batteries to validate the proposed modeling and control strategy. The Flicker meter simulated in the PSCAD/EMTD is used to measure the short term flicker severity index P_{st}. The values of P_{st} obtained without compensator and with compensator are shown in Table-1. Fig. 13 through 16 shows the real power and reactive power from the source before compensation and after compensator DSTATCOM coupled with BESS and not coupled with BESS. The Short Time flicker severity index (Pst) for three different cases are s shown in Table-I.

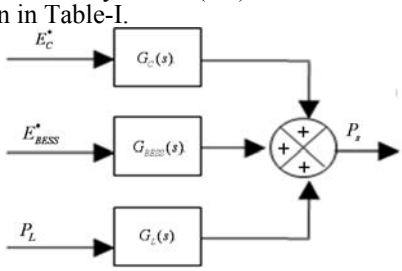

Fig. 11: Simplified block diagram

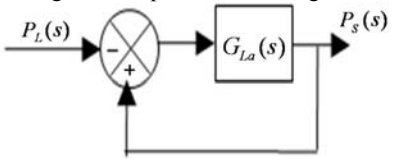

Fig. 12: Source power regulation loop

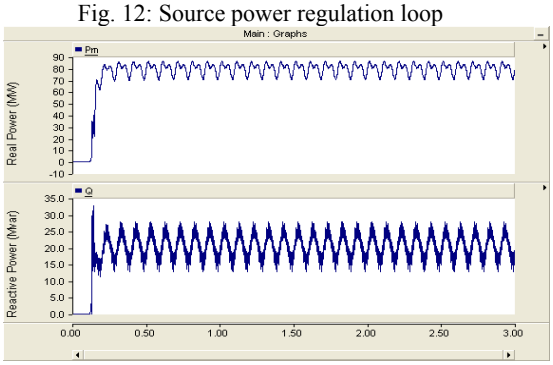

Fig. 13: Real Power and Reactive Power from Source without Compensation

Table 1: Flicker severity index

Compensation strategy	Pst
No compensation means	5.6
Compensation with DSTATCOM without BESS	1.35
Compensation with DSTATCOM with BESS	0.78

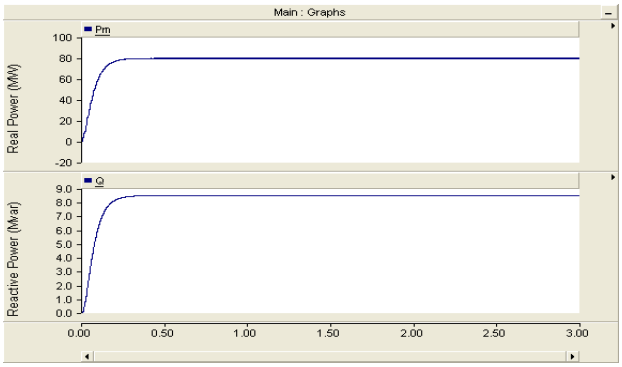

Fig. 14: Real Power and Reactive Power from Source with DSTATCOM and BESS

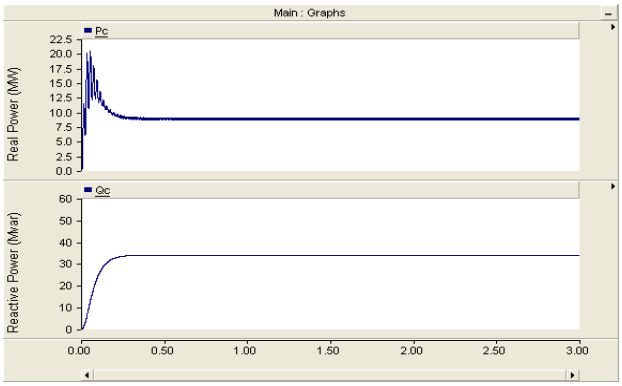

Fig. 15: Real Power and Reactive Power from Source with DSTATCOM and BESS

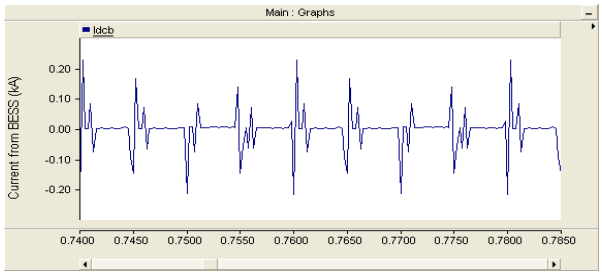

Fig. 16: Current from BESS

VI. CONCLUSION

The paper describes mitigation of flicker due to electric arc furnace by means of DSTATCOM with Battery Energy Storage System (BESS).

In the investigations performed here, the flicker, as indicated by the P_{st} value of the PCC voltage, was initially 5.6 without compensation. The system with DSTATCOM (without BESS) Pst equals to 1.35, indicating the reduction of flicker by 75 % and with DSTATCOM and BESS Pst is 0.78 indicating the reduction in flicker nearly negligible and inconformity with IEEE 1453. It indicates that mitigation of flicker with DSTATCOM and BESS is more effective than DSTATCOM alone by supporting the active and reactive power at the same time. In this paper, the

authors presented the modeling and control strategy of the DSTATCOM/BESS for mitigation of voltage flicker.

APPENDIX

$$G_C(s)=\frac{K_{P1}s^3+\left(K_{P1}K_{P2}+K_{I1}\right)s^2+K_{P1}K_{P2}s}{s^3+\left(K_{P1}+K_{P2}+K_{P3}K_{P2}\right)s^2+\left(K_{I1}+K_{P1}K_{P2}\right)s+K_{P1}K_{P2}} \quad \text{(A1)}$$

$$G_{BESSC}(s)=\frac{K_{P1}K_{P2}s^2+K_{P1}K_{P2}s}{s^{32}+\left(K_{P1}+K_{P2}+K_{P3}K_{P2}\right)s^2+\left(K_{I1}+K_{P1}K_{P2}\right)s+K_{P1}K_{P2}} \quad \text{(A2)}$$

$$G_L(s)=\frac{K_{P1}s^2+\left(K_{P1}K_{P2}+K_{I1}\right)s+K_{I1}K_{P2}}{s^{32}+\left(K_{P1}+K_{P2}+K_{P3}K_{P2}\right)s^2+\left(K_{I1}+K_{P1}K_{P2}\right)s+K_{P1}K_{P2}} \quad \text{(A3)}$$

REFERENCES

[1] Chong Han, Z. Yang, Bin Chen, Alex Q. Huang, Bin Zhang, Mike ingram, Aty Edris, "Evaluation of cascade-multilevel converter based STATCOM for arc furnace flicker mitigation", IEEE IAS'2005, Vol. 1, Oct 2005, pp 67-71.

[2] M. K. Walker, "Electric Utility Limitations", IEEE Trans. Industrial Applications, Vol. 15, Nov. 1979, pp. 644-655.

[3] IEEE Recommended Practices for Measurement and Limits of Voltage Fluctuations and Associated Light Flicker on AC Power Systems, IEEE Standard 1453-2004.

[4] N. G. Hingorani, "Introducing custom power," IEEE Spectrum, Vol. 1, No. 6, Jun 1995, pp. 41-48.

[5] Antonio Moreno-Munoz (Ed) "Power Quality Mitigation Technologies in a Distributed Environment" Springer-Verlag London Limited 2007.

[6] Tongxin Zheng, E. B. Makaram, "An Adaptive arc furnace model", IEEE Trans on Power Delivery, Vol. 15, No. 3, July 2000, pp. 931-939.

[7] S. Vardan, E. B. Makaram, A. A. Girgis, "A new time domain voltage source model for an arc furnace using EMTP", IEEE Trans on Power Delivery, Vol. 11, No. 3, July 1996, pp. 1685-1691.

[8] G. C. montanari, M. Loggini, A. Cavallini, I. Pitti, and D. Zanienlli, "Arc furnace model for study of flicker compensation in electrical networks," IEEE Trans. On Power delivery, Vol. 9, No. 4, October 1994, pp.2036-2033.

[9] Li Zhang, Yilu Liu, Michael R. Ingram, Dale T. Bradshaw, Stev Eckroad, and Mariesa L. Crow, "EAF Voltage Flicker Mitigation By FACTS/ESS," Power System Conference & Exposition, Vol. 1, Oct. 2004, pp. 372-378.

[10] IEEE Recommended Practices for Harmonic Control in Electric Power Systems, IEEE Standard 519-1992, 1993, pp. 80-82.

[11] J. C. Das "Passive Filterss- potentialities and limitations", IEEE Trans on IAS, Vol. 40, No. 1, Jan. 2004, pp-232-241.

[12] Chong Han, Zhanoning Yang, Bin Chen, Alex Q. Haung, Bin Zhang, Michael Ingram, Abdel-Atey, "valuation of Cascade-Multilevel-Converter-Based STATCOM for Arc Furnace Flicker Mitigation," IEEE Trans. On Industry Application, Vol. 43, No.2, March-April 2007.

[13] Aurelio Garcia-Gerrada, Pablo Garcia-Gonzalez, Rafael Collantes, "Comparison of Thyristor-Controlled Reactor and Voltage Source Inverters for Compensation of Flicker Caused by Arc furnaces," IEEE Trans Power Delivery, Vol. 15, October 2000, pp. 1225-1231.

[14] E. Acha, V. Agelidis, O. Anaya-Lara, and T. Miller, "Power Electronics Control in Electrical System, 1st Ed. United Kingdom: Newness, 2002.

[15] Z. Yang, C. Shen, L. Zhang, M. L. Crow and S. Arcitty, "Integration of a STATCOM and Battery Energy Storage", IEEE Trans Power System, Vol. 16, May 2001, pp. 254-260.

[16] P. C. Krause, "Analysis of Electric Machinery", New York: Mc Graw-Hill, 1992, pp. 133-163.

[17] Ziyad Salameh, Margaret A. Casacca, William A. Lynch, "A mathematical model for lead-acid batteries", IEEE Trans on Energy Conversion, Vol. 7, No. 1, march 1992, pp. 93-98 on Energy Conversion, Vol. 17, No. 1, 2002, pp. 16-23.

[18] D. Casadei, G. Grandi, U. Reggiani, C. Rossi, "Active AC line conditioner for a cogeneration system", European Confer. On Power Electronics and Applications, EPE, Lausanne (CH), September 7-9, 1999.

BIOGRAPHIES

Vasudeo B. Virulkar received the B.E. degree in electrical engineering from the Nagpur University, Nagpur (M.S.), India, in 1991, the M.E. (EPS) degree from the Amravati University, Amravati, India, in 1997. After his post graduation, he worked as a Lecturer in Electrical Engineering at Department of Higher and Technical Education, Govt. of Maharashtra and worked at various institutions. Presently, he is working as Lecturer in Electrical Engineering at Govt. College of Engineering, Amravati (M.S.), India and pursuing his research on Power Quality at Department of Electrical Engineering, Visvesvaraya National Institute of Technology, NAGPUR (INDIA) under the guidance of Prof. M. V. Aware.

Mohan V. Aware received the B.E. degree in electrical engineering from the Government College of Engineering, Amravati (M.S.), India, in 1980, the M.Tech. degree from the Indian Institute of Technology, Bombay, India, in 1982, and the Ph.D. from Visvesvaraya Regional College of Engineering, Nagpur, India, in 2002. After his post graduation, he worked as a Design Officer with Crompton Greaves Ltd., Nasik, India from 1982 to 1989. From 1989 to 1991, he was a Development Engineer with Nippon Denro Ispat, Nagpur, India. In 1991, he joined the Electrical Engineering Department, Visvesvaraya Regional College of Engineering, as a Lecturer. Since 1994, he has been with the Power System Research Laboratory, Visvesvaraya Regional College of Engineering as a Scientist "C." From 2001 to 2003, he was a Research Associate with the Electrical Engineering Department, Hong Kong Polytechnic University, Kowloon, Hong Kong. Presently, he is working as a Professor in Electrical Engineering Department at Visvesvaraya National Institute of Technology, NAGPUR (INDIA). He is member of Bureau of Energy Efficiency (BEE) and also recognized Energy Auditor.